Fluid Dynamics, Vol. 29, No. 2, 1994

ON THE APPLICABILITY OF SOME APPROXIMATE SIMILITUDE LAWS IN HYPERSONIC AERODYNAMICS

N. N. Pilyugin, R. F. Talipov, and S. V. Utyuzhnikov

UDC 533.6.011.55

The range of applicability of some similitude laws for heat transfer, friction and drag coefficients is discussed on the basis of numerical solutions of the complete viscous shock layer equations describing hypersonic flow past blunt bodies.

The method of matched asymptotic expansions [1] is used widely in the theory of hypersonic flow past bodies; this method enables one to solve simplified gasdynamic equations in the first terms of the expansion of the unknown functions in asymptotic series in terms of a small parameter [2—4]. Similitude relations for the shock wave stand-off distance, the drag and friction coefficients, the convective and radiative heat transfer to impermeable bodies, which are of practical importance, have been obtained in the last few years on the basis of these solutions [2—5]. In the case of the intense subsonic injection of a foreign gas from the body surface, another small parameter appears, namely, the momentum ratio for the injected and oncoming gases [6, 7]. In this case it is also possible to construct an asymptotic solution and to obtain, for example, the shape of the contact surface separating two flows [7].

The results of asymptotic and numerical studies of supersonic viscous nonuniform wake-type flows past blunt bodies with and without gas injection from the body surface were reviewed in [8].

Since the convergence of asymptotic solutions in the general case of nonlinear gasdynamic equations has not been proved strictly from the mathematical standpoint, the problem of the accuracy and the applicability range of the approximate similitude relations thus obtained arises. In order to arrive at an answer to this problem, it would be well to carry out a systematic comparison with the results of either specifically designed aerodynamical experiments or numerical solutions of the more accurate (non-simplified) gasdynamic equations.

In recent years a numerical method of solving the complete viscous layer equations has been developed [9]. This makes it possible to calculate the distributions of all the gasdynamic parameters in the shock layer adjacent to a blunt cone with or without gas injection from the body surface, in uniform and nonuniform oncoming streams [10—12]. Comparison of the numerical solutions for flow past a sphere and a blunt cone obtained by this method with the experimental data and other numerical and asymptotic solutions [10—12] shows that the method possesses high accuracy and requires less computation time than time-dependent methods for the Navier-Stokes equations. On the basis of the approximate asymptotic solutions, a general similarity law was derived in [13] for convective heat transfer to the side surface of a slender blunt body in laminar hypersonic flow, as well as for other gasdynamic parameters. The similitude laws for inviscid flow past blunt slender bodies and viscous flow past sharp slender bodies follow from this law as special cases.

1. PROBLEM FORMULATION AND NUMERICAL METHOD OF SOLUTION

Steady-state supersonic viscous perfect-gas flow past a smooth axisymmetric body at zero incidence is considered. The non-dimensional free-stream parameters have the form [8]:

$$V_1(r) = 1 - a\exp(-br^2), \quad p_1(r) = 1/(\gamma M_\infty^2), \quad \rho_1(r) = \frac{1 + C\,[1 - (1-a)^{-2}]}{1 + C\,[1 - V_1^2(1-a)^{-2}]} \tag{1.1}$$

Here, rR_0 is the distance from the axis of symmetry and R_0 is the scale-length; V_1V_0, $\rho_1\rho_\infty$, $p_1\rho_\infty V_\infty^2$ are the free-stream dimensional velocity, density, and pressure; γ is the specific heat ratio, and a, b, and c are the nonuniformity parameters. The subscript "∞" relates to the values of parameters as $r\to\infty$.

Moscow. Translated from Izvestiya Rossiiskoi Akademii Nauk, Mekhanika Zhidkosti i Gaza, No.2, pp. 121-130, March-April, 1994. Original article submitted September 21, 1992.

In the orthogonal reference frame fitted to the body surface the viscous shock layer equations have the form [11]:

$$\frac{\partial}{\partial x}(r\rho u)+\frac{\partial}{\partial y}(H_1\rho vr)=0$$

$$\rho\left(\frac{u}{H_1}\frac{\partial u}{\partial x}+v\frac{\partial u}{\partial y}+\frac{uv}{H_1}\right)=-\frac{1}{H_1}\frac{\partial p}{\partial x}+\frac{1}{\mathrm{Re}_\infty H_1^2 r}\frac{\partial}{\partial y}\left(H_1^2 r\mu\left(\frac{\partial u}{\partial y}-\frac{u}{H_1 R}\right)\right)$$

$$\rho\left(\frac{u}{H_1}\frac{\partial v}{\partial x}+v\frac{\partial v}{\partial y}-\frac{u^2}{RH_1}\right)=-\frac{\partial p}{\partial y},\quad \rho\left(\frac{u}{H_1}\frac{\partial H}{\partial y}+v\frac{\partial H}{\partial y}\right)=\frac{1}{\mathrm{Re}_\infty H_1 r}\frac{\partial}{\partial y}\times$$

$$\times\left(H_1 r\frac{\mu}{\mathrm{Pr}}\left(\frac{\partial H}{\partial y}+\frac{\mathrm{Pr}-1}{2H_\infty}\frac{\partial u^2}{\partial y}V_\infty^2-\frac{\mathrm{Pr}\,u^2V_\infty^2}{RH_1H_\infty}\right)\right),\quad H_1=1+\frac{y}{R_0},\quad \mathrm{Pr}=\frac{C_p\mu\mu_\infty}{\lambda},\quad \mathrm{Re}_\infty=\frac{\rho_\infty V_\infty R_0}{\mu_\infty} \tag{1.2}$$

Here, xR_0 and yR_0 are the coordinates along the body surface and normal to it, uV_∞ and vV_∞ are the velocity projections on the x and y axes, $\rho\rho_\infty$, $p\rho_\infty V_\infty^2$, HH_∞, and $\mu\mu_\infty$ are the dimensional density, pressure, total enthalpy, and viscosity; Pr is the Prandtl number, Re_∞ is the Reynolds number, H_1 is the scale factor, and RR_0 is a radius of curvature of the body surface. It is also necessary to add the state equation and the viscosity law to Eqs. (1.2).

Equations (1.2) describe the outer inviscid flow in the shock layer together with the boundary layer flow up to second order in the square root of the reciprocal of the characteristic Reynolds number. The system of equations (1.2) is not wholly parabolic so that well-known marching methods may be used to solve it. However, the Cauchy problem for this system is not correct in the subsonic region [9—11]; this leads to significant difficulties in using any step-by-step technique directly. Therefore, various methods of regularization have sometimes been used (see [9, 10]). A numerical method for solving of the complete steady-state viscous shock layer equations was proposed in [9—12]; this method uses the step-by-step procedure repeated many times, together with refinement of the shock shape and the pressure field at every stage of the global iteration. It would considerably reduce the required computation time and memory.

Let us go over to the new independent variables ξ and η and to the stream function f in Eqs. (1.1), (1.2)

$$\xi=x,\quad \eta=\frac{1}{\Delta}\int_0^y\rho r'dy,\quad r'=1+\frac{y\cos\alpha}{r_w},\quad \Delta=\int_0^{y_s}\rho r'dy,\quad f=\frac{\Psi}{2\pi\rho_\infty V_\infty r_w\Delta\cos\alpha} \tag{1.3}$$

Here, r_wR_0 is the distance from the body contour to the axis of symmetry, y_sR_0 is the stand-off shock wave distance, and α is the angle between the tangent to the body generator and the axis of symmetry. The system of equations (1.2) in the variables ξ and η is given in [11, 12].

The slip and temperature jump conditions are assumed at the body surface [11]; in the variables ξ, η these conditions are as follows (for $\eta=0$):

$$v=0,\quad u=\frac{a_1\mu}{\mathrm{Re}_\infty\Delta}\sqrt{\frac{\rho}{p}}\left(\frac{\partial u}{\partial\eta}-\frac{\Delta}{\rho}\frac{u}{R}\right)$$

$$H=h_w+\frac{b_1}{\Delta}\frac{\mu}{\mathrm{Re}_\infty}\sqrt{\frac{\rho}{p}}\frac{\partial}{\partial\eta}\left(H-\frac{u^2V_\infty^2\cos^2\alpha}{2H_\infty}\right)+\frac{u^2V_\infty^2\cos^2\alpha}{2H_\infty},\quad a_1=1.2304,\quad b_1=2.3071 \tag{1.4}$$

Here, $uV_\infty\cos\alpha$ and vV_∞ are the velocity vector projections on the x and y axes. Generalized Rankine—Hugoniot relations with slip taken into account were assumed at the shock. These relations for the case of a nonuniform oncoming stream can be derived in the same way as in [11]. We will give the final formulas, without derivation, in the variables ξ, η (for $\eta=1$):

$$C_1\frac{\partial u}{\partial\eta}+u+(1-k_s)C_2\cos\alpha-V_1\cos\alpha-\frac{\cos^2\beta\cos\beta_s}{\mathrm{Re}_\infty\rho_1V_1\sin\beta}\frac{dV_1}{dr}=0$$

$$\frac{C_1}{\cos^2\beta_s\mathrm{Pr}}\frac{\partial H}{\partial\eta}+H-1+\frac{V_\infty^2}{H_\infty}\left(1-\frac{1}{\mathrm{Pr}}\right)\left\{C_1u\frac{\partial u}{\partial\eta}-\frac{V_1\cos^3\beta}{\mathrm{Re}_\infty}\frac{dV_1}{dr}\right\}=0 \tag{1.5}$$

$$p_s = (\gamma M_\infty^2)^{-1} + (1 - k_s)\,\rho_1 V_1^2 \sin^2\beta\,,\quad C_1 = \frac{\mu p r' \cos^3\beta_s}{\Delta\,\mathrm{Re}_\infty\,\rho_1 V_1 \sin\beta}\,,\quad C_2 = \frac{\sin\beta\sin\beta_s}{\cos\alpha}$$

$$k_s = \frac{\rho_1}{\rho_s} = \frac{\gamma - 1}{\gamma + 1} + \frac{2}{(\gamma + 1)\,\rho_1 V_1^2 M_\infty^2 \sin^2\beta}\,,\quad \beta_s = \beta - \alpha$$

Here, β is the angle between the tangent to the shock surface and the axis of symmetry. The subscript "s" relates to the shock parameters.

In the new variables the shock stand-off distance Δ can be determined from the mass balance equation and expressed as follows:

$$\Delta = \frac{(1 + F)\,r_w}{(f_s - I)\,2\cos\alpha}\,,\quad I = \int_0^1 \frac{d\eta}{\rho}\,,\quad F(r_s) = \frac{B(1 - a)^2}{2bCr_w^2}\ln\left\{ \left|\frac{\alpha_0 - W_1}{\alpha_0 - W_0}\right|^{\alpha_0 - 1} \left|\frac{\alpha_0 + W_0}{\alpha_0 + W_1}\right|^{\alpha_0 + 1}\right\},$$

$$W_1 = V_1(r_s),\quad W_0 = 1 - a,\quad \alpha_0 = (1 - a)\sqrt{\frac{1 + C}{C}}\,,\quad r_s = r_w + y_s\cos\alpha \qquad (1.6)$$

We shall also use the geometric relation

$$\mathrm{tg}\,\beta_s = \frac{1}{H_{1s}}\frac{dy_s}{dx}\,,\quad H_{1s} = 1 + \frac{y_s}{R} \qquad (1.7)$$

The formulas from [12] were used as the initial approximation to the shock shape

$$\mathrm{tg}\,\beta_s = D\left(\sqrt{\mathrm{tg}^2\,\alpha + \frac{2D - 1}{D^2}} - \mathrm{tg}\,\alpha\right)$$

$$D = \frac{R_{s0}}{2R_0 H_{1s0}}\,,\quad H_{1s0} = 1 + \frac{y_s(0)}{R_0}\,,\quad D = \frac{1.05 + 1.65k_{s0}}{2(1 + 0.78k_{s0})}\,,\quad k_{s0} = \frac{\rho_\infty}{\rho_{s0}} \qquad (1.8)$$

The calculations were carried out over the following range of the free-stream parameters: $\gamma=1.4$, $\omega=0.5$—1, $M_\infty \geq 6$, $10^2 \leq \mathrm{Re}_\infty \leq 10^6$, $0.01 \leq T_w \leq 1$, $f_w=0$, ω being the exponent in the viscosity law $\mu \sim T^\omega$. For the most part, the nonuniformity parameters b and C had fixed values: $b=7.2$, $C=3.0$. The parameter a varied over the range $0 \leq a \leq a_*$, $a_*(b, C, M_\infty, \mathrm{Re}_\infty, T_w)$ being the critical value characterizing the transition to separation flow on the body nose.

The calculations were performed using nonuniform grids. Thirty grid points were prescribed across the shock layer and approximately one half of these lay within the boundary layer. The calculations along the body were carried out by the block-marching technique. The blocks, which contained from 20 to 25 grid points in the longitudinal coordinate, were calculated sequentially up to convergence. A high order-of-accuracy scheme similar to that of [11] was used in the numerical solution.

The difference equations having been solved, the distributions of the heat flux q_w and the friction coefficient C_f were calculated using the following formulas:

$$q_w = \frac{\rho\mu}{\mathrm{Pr}\,\mathrm{Re}_\infty}\frac{\partial H}{\partial\eta}\,,\quad C_f = \frac{2\rho\mu\cos\alpha}{\mathrm{Re}_\infty}\frac{\partial u}{\partial\eta}\quad (\eta = 0)$$

Here, the heat flux has been divided by $\rho_\infty V_\infty H_0$, and the friction force by $\rho_\infty V_\infty^2/2$.

The main parameters governing the flow in the injection layer [6, 7] are the relative mass flow rate $G_w(\rho_w^*, v_w^*)$ and the momentum density ratio δ of the injected and oncoming gases, where ρ_w^* and v_w^* are the characteristic density and velocity in the injected gas

$$G_w = \frac{\rho_w^* v_w^*}{\rho_\infty V_\infty}\,,\quad \delta = \left(\frac{\rho_w^* v_w^{*2}}{\rho_\infty V_\infty^2}\right)^{1/2}$$

The values of these parameters are presented below.

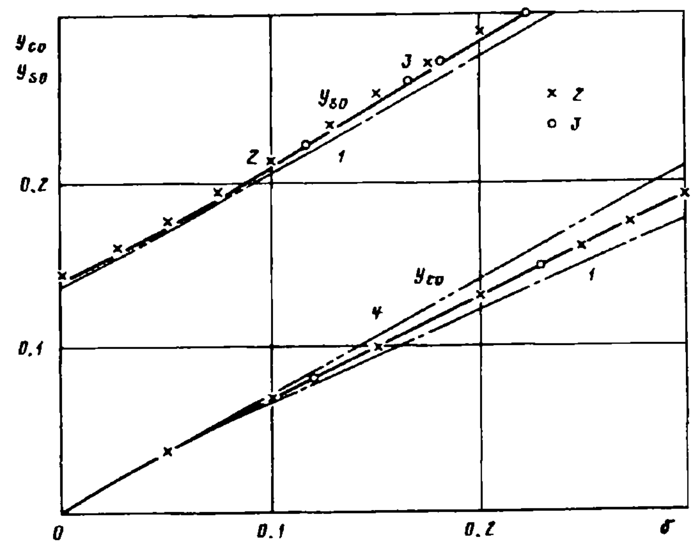

Fig 1

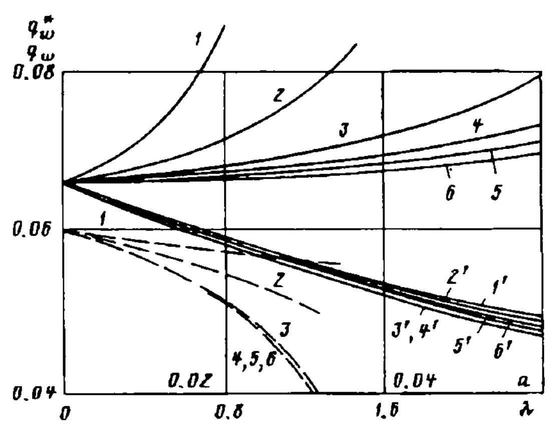

Fig 2

2. RESULTS OF CALCULATIONS IN THE NEIGHBORHOOD OF THE STAGNATION LINE

Let us consider some results of comparing the numerical solution of this paper and the asymptotic solutions for uniform supersonic flow with parameters $M_\infty = 10$, $Re_\infty = 10^4$, $\gamma = 1.4$ past a spherical bluntness. The temperature factor $T_w/T_0 = 0.571$ and the Prandtl number $Pr = 0.72$. The viscosity coefficient was determined using a power law with exponent $\omega = 0.75$.

Figure 1 presents plots of the shock wave stand-off distance on the axis of symmetry y_{s0} and the thickness of the injection layer y_{c0} against the parameter δ.

The continuous curves relate to the present work. The results of calculating the Euler equations by the time-dependent method [15] and the Navier—Stokes equations [14] are shown by curves 1 and the symbols 2, respectively. The experimental data obtained in [16] are numbered 3 in Fig. 1. The shock stand-off distance y_{s0} and the position of the separating streamline y_{c0} determined using the Euler equations lie somewhat lower than the experimental points [16] and the calculated results with viscosity taken into account. The results of the numerical solutions of the Navier—Stokes equations and of the complete viscous layer equations almost coincide with the experimental data. Curve 4 represents the thickness of the injection layer calculated in accordance with the formulas of [7]. The analytical solution of [7] has good accuracy for $0 \leq \delta \leq 0.1$, but with increase in the injection strength (for $\delta > 0.1$) it overestimates y_{c0} — by approximately by 6% as compared with the experimental data and the

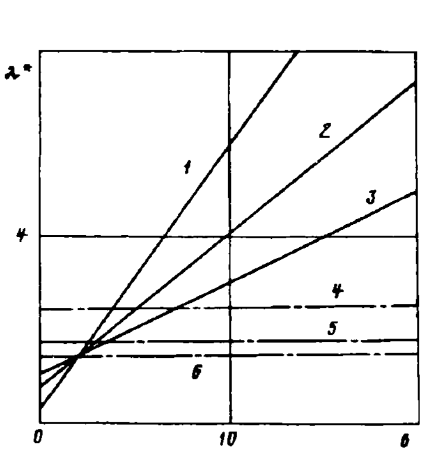

Fig 3

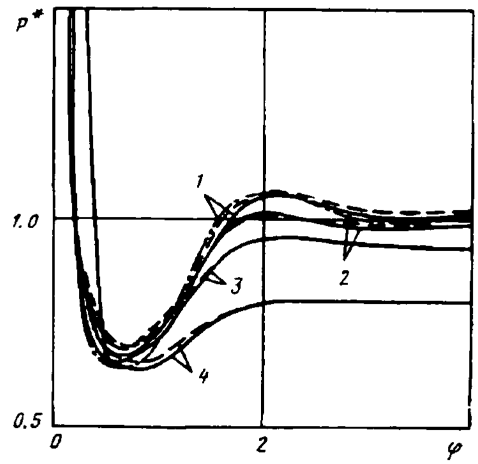

Fig 4

calculated results with viscosity taken into account, and by 15—18% as compared with the solution of the Euler equations.

3. VERIFICATION OF THE SIMILITUDE RELATIONS FOR NONUNIFORM FLOW

As shown in [8, 17, 18], when the thin (hypersonic) viscous shock layer model is used, the effect of the wake-like nonuniformity in the oncoming stream manifests itself in the neighborhood of the stagnation streamline through the parameter $\lambda=2ab(1+C)/(1-a)$, which enters into the expansion of the pressure gradient $\partial p/\partial x$ in the powers of x. However, the calculations using Eqs. (1.2) show that the parameter λ cannot be used as the similitude criterion in the nonuniform far-wake-like flow past blunt bodies. Figure 2 presents as an example the dependence of the heat flux q_w^* on the parameter λ for $M_\infty=20$, $Re_\infty=10^4$, $T_w/T_0=0.1$. Here, the heat flux is nondimensionalized by the density and velocity on the axis of symmetry in the nonuniform oncoming stream [18]

$$q_w^* = \frac{q_w}{(1-a)\{1+C\,[1-(1-a)^{-2}]\}} \tag{3.1}$$

Curves 1—6 correspond to the values of the parameter $b=1.7$, 3.05, 5.4, 7.2, 9.6, and 12.8, for $C=3.0$. The continuous curves represent the solution of equations (1.2), while the broken ones represent the solution of the thin viscous-layer equations. With decrease in the parameter b ($b<3.0$) the heat flux plots begin to diverge. At the same time, the plots $q_w(a)$ represented by the curves 1′—6′ in Fig. 2, which correspond to the solution of equations (1.2) for the same values of the parameter b, diverge only slightly. In both cases the plots $q_w(a)$ are monotonic decreasing. As for the dissimilarity of the dependence $q_w^*(\lambda)$, it is due, firstly, to a faster decrease in q_w^* with increase in nonuniformity (i.e., the parameter a) for the case of a thin viscous shock layer, which is connected with the assumption of an equidistant shock and body; and, secondly, to the non-dimensionalizing, in accordance with (3.1), by the product $B(1-a)$, which varies with a.

Thus, using the nonuniformity parameter a gives some advantages as compared to the parameter λ. That is why in what follows the parameter a is assumed to be the main parameter of nonuniformity.

In [18] it was proposed that the criterion of transition to the separation flow regime in the form $\lambda_*=\lambda_*(Re_\infty, M_\infty, T_w)$ be used instead of the criterion $a_*=a_*(b, C, Re_\infty, M_\infty, T_w)$ considered in [17]. Figure 3 presents the plots of λ_* against the parameter b averaged over some values of the parameter C (from the range $C=3$—5) for various Reynolds numbers. Curves 1 and 4 correspond to $Re_\infty=10^2$, curves 2 and 5 to $Re_\infty=10^3$, and curves 3 and 6 to $Re_\infty=10^5$. The continuous and chain curves relate to the calculations for the complete viscous shock layer and for the thin viscous shock layer according to [8]. It can be seen from Fig. 3 that the parameter C influences the value of λ_* only slightly. The values of λ_* obtained in accordance with the viscous shock layer model (chain lines) are almost independent of b and C at fixed Reynolds numbers. As $Re_\infty\to\infty$, the asymptotic value of $\lambda_*=4/3$ obtained in [18] becomes quite accurate. The calculations made using the complete viscous shock layer model lead to a linear dependence of λ_* on the parameter b at a fixed Reynolds number Re_∞. The exact model, taking the disturbance transfer upstream into account, shows that the criterion $\lambda_*=\text{const}$ [18] leads to erroneous results for separation

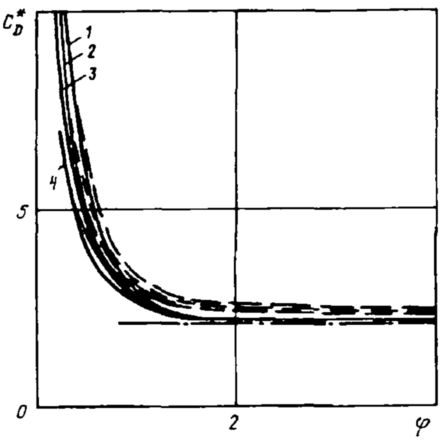

Fig 5

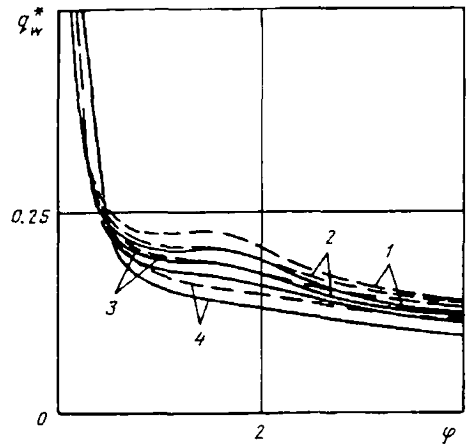

Fig 6

in the nonuniform flow.

4. ON THE SIMILITUDE RELATIONS FOR SLENDER BLUNT CONES

The hypersonic inviscid gas flow theory for slender blunt bodies (wedges and cones) gives asymptotic similitude laws [2, 3] consisting in the fact that for affinely similar bodies, independently of the bluntness shape, the relative pressure on the body p^*, the shock slope χ, and the drag coefficient C_D^* depend on three non-dimensional variables: γ, $k=M_\infty \tan\alpha_c$, φ

$$p^* = \frac{p_w - p_0}{\mathrm{tg}^2\,\alpha_c}, \quad \chi = \frac{\mathrm{tg}\,\beta}{\mathrm{tg}\,\alpha_c}, \quad C_D^* = \frac{C_D}{\sin^2\alpha_c}, \quad \varphi = \sqrt{\frac{2}{C_{D0}}}\,\mathrm{tg}^2\,\alpha_c x$$

Here, C_{D0} is the drag coefficient of the body bluntness.

In accordance with [13], in the case of hypersonic laminar flow past slender blunt bodies, if the following similitude criteria are equal

$$\gamma,\ k,\ \varphi,\ \frac{h_w H_0}{V_\infty^2}, \quad \Omega = \frac{M_\infty^2 \mu_0}{\mathrm{Re}_\infty}\sqrt{\frac{2}{C_{D0}}}$$

(here, H_0 and V_∞ are the dimensional total enthalpy and velocity, μ_0 is the viscosity coefficient at the stagnation point), then the functions p^*, χ, C_D^* and q_w^* are constant, where

$$q_w^* = \frac{q_w}{\sqrt{\Omega}\,\mathrm{tg}^3\,\alpha_c}\left(\frac{1}{2} + \frac{1}{(\gamma - 1)M_\infty^2}\right)$$

In this case the equality of γ, k, and φ ensures the similarity of the inviscid flows, while the equality of $h_w H_0/V_\infty^2$ and Ω ensures the similarity of the boundary layers.

Figures 4, 5, and 6 present plots of p^*, C_D^*, and q_w^* against the similitude parameter φ for the fixed values $\gamma=1.4$, $k=3.5$, and $h_w H_0/V_\infty^2=0.0525$. The continuous curves relate to the parameter $\Omega=6.51\cdot10^{-4}$, and the broken curve to $\Omega=5.9\cdot10^{-2}$. Viscosity was determined in accordance with a power law $\mu \sim T^\omega$ with exponent $\omega=0.5$. Curves 1—4 correspond to the cone half-angles $\alpha_c=10$, 15, 20, and 30°. The chain curve in Fig. 4, taken from [19], relates to inviscid gas flow past a cone with spherical bluntness and half-angle $\alpha_c=10°$, for $M_\infty \to \infty$ and $\gamma=1.4$. The $p=p(\varphi)$ curves for $\alpha_c \leq 20°$ are similar regardless of the similitude parameter Ω. For $\alpha_c=30°$ the values of p^* are essentially lower, since the assumption of a slender body is too rough in this case. The relative values of C_D^* as functions of φ are similar even at $\alpha_c=30°$ (Fig. 5). In the case of low values of the parameter Ω with growing φ the plots of C_D^* tend to the limiting value, which was obtained numerically using the plane cross-sections law [2] (this value is indicated by the chain line in Fig. 5). The plots of the relative heat flux q_w processed using the parameter Ω are close to each other at $\alpha_c \leq 20°$ (Fig. 6), though the initial values of q_w for various Ω differ by more than two orders of magnitude. For small cone angles ($\alpha_c \leq 10°$) the plots of q_w^* have maxima at $\varphi \approx 1.5$ due to the effect of entropy layer absorption. A well-defined maximum can be observed in the pressure distribution at $\varphi=2.0$ (Fig. 4).

Thus, a comparison of the approximate similitude relations and the numerical solutions makes it possible to clarify the range of applicability of these relations, while the similitude parameters proposed in [2, 6, 13] turn out to be useful in the processing of the results of numerical calculations.

REFERENCES

1. M. D. Van Dyke, *Perturbation Methods in Fluid Mechanics*, New York (1964).
2. G. G. Chernyi, *Gas Flows at High Supersonic Velocities* [in Russian], Fizmatgiz, Moscow (1959).
3. V. V. Luniov, *Hypersonic Aerodynamics* [in Russian], Mashinostroenie, Moscow (1975).
4. W. D. Hayes and R. F. Probstein, *Hypersonic Flow Theory*, Academic Press, New York (1966).
5. N. N. Pilyugin and G. A. Tirskii, *Dynamics of Ionized Radiating Gases* [in Russian], Moscow University Press, Moscow (1989).
6. É. A. Gershbein, "Hypersonic viscous shock layer theory at high Reynolds numbers and the intense injection of foreign gases," *Prikl. Mat. Mekh.*, **38**, 1015 (1974).
7. N. N. Pilyugin and R. F. Talipov, "Asymptotic solution of the Euler equations in the shock layer on a blunt body in nonuniform flow with gas injection from the body surface," *Izv. Akad. Nauk SSSR, Mekh. Zhidk. Gaza*, No. 6, 126 (1989).
8. I. G. Eremeitsev, N. N. Pilyugin, V. S. Khlebnikov, and S. A. Yunitskii, *Study of Aerodynamic Characteristics and Heat Transfer for Bodies in Nonuniform Supersonic Gas Flows* [in Russian], Moscow University Press, Moscow (1988).
9. S. A. Vasilyevskii, G. A. Tirskii, and S. V. Utiuzhnikov, "Numerical method of solving the viscous shock layer equations," *Zh. Vychisl. Mat. Mat. Fiz*, **27**, 741 (1987).
10. G. A. Tirskii and S. V. Utiuzhnikov, "Comparison of the thin and complete viscous shock layer models in the problem of supersonic viscous gas flows past blunt cones," *Prikl. Mat. Mekh.*, **53**, 963 (1989).
11. N. N. Pilyugin and R. F. Talipov, "Numerical study of nonuniform flow past a sphere within the framework of the viscous shock layer model," *Zh. Prikl. Mekh. Tekh. Fiz.*, No. 5, 62 (1991).
12. S. A. Vasilyevskii and G. A. Tirskii, "Numerical method of solving the viscous shock layer equations," in: *Studies on Hypersonic Aerodynamics and Heat Transfer with NonEquilibrium Chemical Reactions* [in Russian], Moscow University Press, Moscow (1987), p. 5.
13. V. V. Luniov, "The similarity law for hypersonic viscous gas flows past slender blunt bodies," *Prikl. Mat. Mekh.*, **25**, 1050 (1961).
14. Z. M. Emelyanova and B. M. Pavlov, "Calculation of injection from blunt body surfaces in supersonic flow using the complete Navier—Stokes equations," in: *Numerical Methods in the Aerodynamics*, No. 2 [in Russian], Moscow University Press, Moscow (1979), p. 69.
15. M. M. Gilinskii and M. G. Lebedev, "Calculation of intense blowing on a blunt body and an airfoil," *Izv. Akad. Nauk SSSR, Mekh. Zhidk Gaza*, No. 1, 117 (1977).
16. E. D. Katzen and G. E. Kaattari, "Inviscid hypersonic flow around blunt bodies," *AIAA J.*, **3**, 1230 (1965).
17. I. G. Eremeitsev and N. N. Pilyugin, "Heat transfer and drag of a body in a far supersonic wake," *Izv. Akad. Nauk SSSR, Mekh. Zhidk Gaza*, No. 2, 60 (1986).
18. S. V. Peigin and S. V. Timchenko, "Hypersonic three-dimensional viscous shock layer in a nonuniform gas flow in the neighborhood of the stagnation point," *Izv. Akad. Nauk SSSR, Mekh. Zhidk Gaza*, No. 6, 136 (1987).
19. M. M. Gilinskii, M. G. Lebedev, and I. R. Yakubov, *Simulation of Gas Flows with Shock Waves* [in Russian], Mashinostroenie, Moscow (1984).